



# Prostate cancer therapy using immune checkpoint molecules to target recombinant dendritic cells

Se Young Choi<sup>1,\*</sup> , Yunlim Kim<sup>2,3,\*</sup> , Bumjin Lim<sup>3</sup> , Chung Beum Wee<sup>1</sup> , In Ho Chang<sup>1</sup> , Choung-So Kim<sup>4</sup>

<sup>1</sup>Department of Urology, Chung-Ang University Hospital, Chung-Ang University College of Medicine, Seoul, <sup>2</sup>Asan Institute for Life Sciences, Asan Medical Center, Seoul, <sup>3</sup>Department of Urology, Asan Medical Center, University of Ulsan College of Medicine, Seoul, <sup>4</sup>Department of Urology, Ewha Womans University Mokdong Hospital, Ewha Womans University School of Medicine, Seoul, Korea

**Purpose:** We developed immune checkpoint molecules to target recombinant dendritic cells (DCs) and verified their anti-tumor efficacy and immune response against prostate cancer.

**Materials and Methods:** DCs were generated from mononuclear cells in the tibia and femur bone marrow of mice. We knocked down the programmed death ligand 1 (PD-L1) on monocyte-derived DCs through siRNA PD-L1. Cell surface antigens were immune fluorescently stained through flow cytometry to analyze cultured cell phenotypes. Furthermore, we evaluated the efficacy of monocyte-derived DCs and recombinant DCs in a prostate cancer mouse model with subcutaneous TRAMP-C1 cells. Lastly, DC-induced mixed lymphocyte and lymphocyte-only proliferations were compared to determine cultured DCs' function.

**Results:** Compared to the control group, siRNA PD-L1 therapeutic DC-treated mice exhibited significantly inhibited tumor volume and increased tumor cell apoptosis. Remarkably, this treatment substantially augmented interferon-gamma and interleukin-2 production by stimulating T-cells in an allogeneic mixed lymphocyte reaction. Moreover, we demonstrated that PD-L1 gene silencing improved cell proliferation and cytokine production.

**Conclusions:** We developed monocyte-derived DCs transfected with PD-L1 siRNA from mouse bone marrow. Our study highlights that PD-L1 inhibition in DCs increases antigen-specific immune responses, corroborating previous immunotherapy methodology findings regarding castration-resistant prostate cancer.

**Keywords:** Dendritic cell; Immune tolerance; Immunotherapy; Prostate cancer

This is an Open Access article distributed under the terms of the Creative Commons Attribution Non-Commercial License (<http://creativecommons.org/licenses/by-nc/4.0>) which permits unrestricted non-commercial use, distribution, and reproduction in any medium, provided the original work is properly cited.

## INTRODUCTION

Prostate cancer is the most prevalent type and the second cause of cancer-specific mortality among men in the United States [1]. New medications have redefined metastatic prostate cancer treatment, bolstering patient survival and quality of life [2]. However, new therapeutic tools are

needed for advanced prostate cancer patients that were non-responsive to previous treatment.

Therapies employing the patient's immune system have garnered considerable attention in the last decade [3]. Immune-checkpoint inhibitors are notably effective for 'hot tumors' such as melanoma and renal cell carcinoma [4,5]. Immunotherapy first ascertains tumor presence [6], and can

**Received:** 19 October, 2023 • **Revised:** 18 January, 2024 • **Accepted:** 11 February, 2024 • **Published online:** 17 April, 2024

**Corresponding Author:** Choung-So Kim <https://orcid.org/0000-0002-7464-3207>

Department of Urology, Ewha Womans University Mokdong Hospital, Ewha Womans University School of Medicine, 1071 Anyangcheon-ro, Yangcheon-gu, Seoul 07985, Korea

TEL: +82-2-3010-3734, FAX: +82-2-6294-1406, E-mail: cskim37345806@gmail.com

\*These authors contributed equally to this study and should be considered co-first authors.

easily attack tumors exhibiting substantial T-cell infiltration, programmed death ligand 1 (PD-L1) expression, and tumor mutation burden [7]. However, immunotherapy's response rate is 10%–35% relative to cancer type [8]. Moreover, only 5%–10% of prostate cancer cases were microsatellite instability-high or mismatch repair-deficient, a potential indicator for durable immunotherapy responses [9]. The tumor microenvironment in prostate cancer also mediates immunosuppression by secreting molecules or influencing cellular interaction [10]; thus, prostate cancer is known as a 'cold tumor.'

Nevertheless, immunotherapy has succeeded in treating prostate cancer. Sipuleucel-T, an autologous active dendritic cellular immunotherapeutic agent, exhibited a significant survival gain in a randomized phase 3 trial concerning metastatic castration-resistant prostate cancer (CRPC) [11]. Dendritic cells (DCs) induce cytotoxic T-cells through tumor antigens and are vital for cancer immunotherapy [12]. We focused on DC's efficacy as an antigen-presenting cell in prostate cancer, hypothesizing that a recombinant gene to avoid immunologic tolerance would reinforce anti-tumor effects in prostate cancer.

## MATERIALS AND METHODS

### 1. Establishing subcutaneous prostate cancer and DC treatment in mice

The Asan Medical Center's Institutional Animal Care and Use Committee (IACUC) reviewed and approved all animal experiments (#020-12-086). The *in vitro* and *in vivo* experiments were conducted at Asan Medical Center. TRAMP-C1 mouse prostate cancer cells at a  $5 \times 10^6$  cells/mouse density were subcutaneously injected into the right flank of male mice six weeks old (Central Lab. Animal Inc.). Treatment began after one week when the tumor volume was approximately  $70 \text{ mm}^3$ . One week post-injection, mice were categorized into four groups: vehicle, mono-DC, prostate specific membrane antigen (PSMA) peptide-pulsed/small interfering RNA (siRNA) PD-L1 treated mono-DC, and cell lysate-pulsed/siRNA PD-L1 treated mono-DC. TRAMP-C1-bearing tumor mice were subcutaneously injected once a week for three weeks with  $5 \times 10^6$  DCs around inguinal lymph nodes for the medium group. Tumor measurements were evaluated thrice per week using calipers and calculated using the following formula: tumor volume ( $\text{mm}^3$ ) = length  $\times$  width<sup>2</sup>  $\times$  0.5 (length is the longest diameter, and width is the shortest diameter perpendicular to length). On Day 76, the tumor growth inhibition ratio (TGI, %) was calculated using the following formula:

### Recombinant dendritic cells for prostate cancer therapy

$$\text{TGI (\%)} = \left[ 1 - \left( \frac{\text{relative tumor volume}_{\text{treated group}}}{\text{relative tumor volume}_{\text{control group}}} \right) \right] \times 100$$

### 2. Monocyte-derived DC generation

DCs were generated from bone marrow mononuclear cells (BM-MNCs) collected from C57BL/6 mice's tibia and femur, passed through a  $40 \mu\text{m}$  nylon mesh cell strainer (Corning) to remove small bones and debris, and resuspended in RPMI 1640 containing 10% fetal bovine serum medium. Cell suspensions in the dish were collected and centrifuged at 1,300 rpm for 10 minutes, and the supernatant was discarded. Then, the cell pellet was resuspended with a 1% Ammonium Chloride (Dongin Biotech) red blood cell (RBC) lysis buffer. Following centrifugation, the supernatant was discarded, and the pelleted cells were washed with phosphate-buffered saline (PBS) and collected. BM-MNCs' myeloid lineage cells were separated using a magnetic bead MACS lineage depletion kit (Miltenyi Biotech). Purified cells were cultured with granulocyte-macrophage colony-stimulating factor (GM-CSF) (1,000 units/mL) and interleukin-4 (IL-4) (1,000 units/mL) (PeproTech).

On Day 5 (Fig. 1), PD-L1 and recommended negative stealth control siRNA duplexes were obtained from Ambion. All siRNAs were dissolved or diluted to a  $25 \mu\text{M}$  concentration in diethylpyrocarbonate (DEPC) water (Thermo Fisher Scientific) and stored at  $-80^\circ\text{C}$ . Cells were transiently transfected with siRNA using the RNA interference max transfection reagent (Thermo Fisher Scientific) for 72 hours following the manufacturer's instructions. messenger RNA (mRNA) and protein levels were detected using real-time quantitative reverse transcription-polymerase chain reaction (RT-PCR) and western blotting to ascertain the target sites' silencing effects.

### 3. Tumor antigen pulsing and DC maturation

One day after pulsing with tumor cell lysate or PSMA Peptivator<sup>®</sup> pulsing peptide (Miltenyi Biotech), lipopolysaccharide (LPS) (Sigma-Aldrich) for DCs were added to the culture media for 24 hours as maturation factors before harvesting. Tumor cell lysates were prepared from cultured TRAMP-C1 cells through a freeze-thaw process repeated seven times in liquid nitrogen ( $\text{LN}_2$ ) and a water bath ( $37^\circ\text{C}$ ). Protein concentrations were measured using the Bradford protein assay (Bio-Rad). Cultured DCs were characterized as DCs through specific phenotyping and DC-induced naïve T-cell proliferation and cytokine secretion.

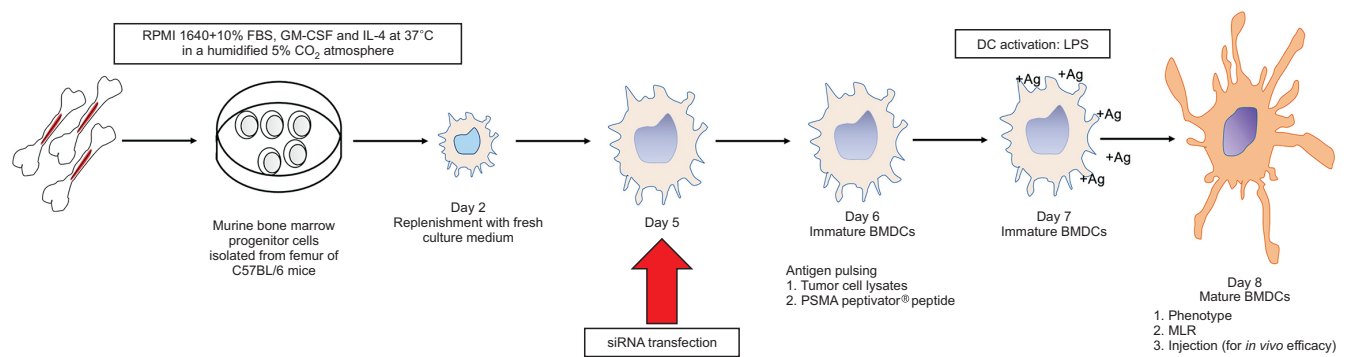


**Fig. 1.** Monocyte-derived DCs generation. DCs were generated from the bone marrow mononuclear cells collected from C57BL/6 mice's tibia and femur. Cells were transfected with PD-L1 stealth siRNA on Day 5. TRAMP-C1 tumor cell lysate or PSMA Peptivator® was added to the culture media two days before harvesting DCs as antigens. LPS was added to the culture media as a DC maturation factor for 18–24 hours before harvesting. DCs, dendritic cells; PD-L1, programmed death ligand 1; siRNA, small interfering RNA; PSMA, prostate specific membrane antigen; LPS, lipopolysaccharide; FBS, fetal bovine serum; GM-CSF, granulocyte-macrophage colony-stimulating factor; IL-4, interleukin-4; BMDCs, bone marrow derived dendritic cells; MLR, mixed lymphocyte reaction.

#### 4. PD-L1-knockdown cultured DCs through western blot

Whole-cell lysates were prepared in a RIPA lysis buffer containing protease inhibitor cocktails (Sigma Aldrich), micro-centrifuged at 13,000×g for 5 minutes, and the supernatants were stored at 4°C. Then, the protein concentration was measured using the Bradford protein assay (Bio-Rad). Equal protein amounts (20 µg in 20 µL) were subjected to sodium dodecyl sulfate-polyacrylamide gel electrophoresis (SDS-PAGE) and transferred to a polyvinylidene fluoride (PVDF; Merck Millipore Ltd.) membrane. After blocking with 5% bovine serum albumin for 1 hour at room temperature, the membranes were first incubated with primary antibodies overnight at 4°C with shaking (100 rpm), then with peroxidase-conjugated secondary antibodies for 1 hour at room temperature. The Immobilon Western enhanced chemiluminescent solution (Millipore) visualized immunoreactive bands on X-ray film (Fujifilm). Lastly, membranes were stripped and re-probed with β-actin antibodies to confirm equal protein loading.

#### 5. PD-L1-knockdown cultured DCs from real-time quantitative RT-PCR

Total RNA was extracted from transfected DCs, and 2 µg aliquots were reverse transcribed using first-strand complementary DNA (cDNA) synthesis kits (Toyobo). The subsequent cDNA samples were subjected to real-time PCR in an ABI 7500 sequence detector system using SYBR Green PCR Master Mix (Toyobo). Each gene's PCR amplification efficiency and linearity were evaluated, including target and control genes. Results were normalized to those of 18s mRNA and quantitatively analyzed using the  $2^{-\Delta\Delta Ct}$  method. The amplification protocol entailed an initial denaturation

at 95°C for 20 seconds, 40 denaturation cycles at 95°C for 3 seconds, and annealing and extension at 60°C for 30 seconds. The melt curve stage included 15 seconds at 95°C, a melt from 60°C for 1 minute to 95°C for 15 seconds with a 1% ramp rate, and 60°C for 15 seconds. Amplification primers comprised those for mouse PD-L1: 5'-CTCATTGTAGTGTC-CACGGTC-3' (forward) and 5'-ACGATCAGAGGGTTCAA-CAC-3' (reverse); and 18s: 5'-AGAAACGGCTACCACATC-CA-3' (forward) and 5'-CCCTCCAATGGATCCTCGTT-3' (reverse).

#### 6. Flow cytometric immunophenotyping analysis of cultured DCs

Cultured cell phenotypes were analyzed through direct immune fluorescence staining of cell surface antigens using fluorescein isothiocyanate (FITC), peridinin-chlorophyll-protein (PerCP), phycoerythrin (PE), or Allophycocyanin (APC) conjugated antibodies against MHC I/II, CD11c, CD80/86 and CD14 (eBioscience) by flow cytometry. Fluorescence-labeled IgG isotypes were selected as the control. All antibodies were used at manufacturer-recommended concentrations.

#### 7. Lymphocyte proliferation assay

Spleens were disaggregated, and cell suspensions were collected in RPMI 1640 culture mediums to discern cultured DC functions using mixed lymphocyte reaction assays. Erythrocytes were eliminated through incubation with a 1% ammonium chloride RBC lysis buffer. Cells were washed with RPMI 1640 medium and passed through a 40 µm nylon mesh cell strainer to obtain a single-cell suspension. Lymphocytes were plated in 96-well plates and exposed to concanavalin A (con A, 25 µg/mL; Sigma-Aldrich). Irradiated/matured (25 Gy) DCs were diluted, added to respond-

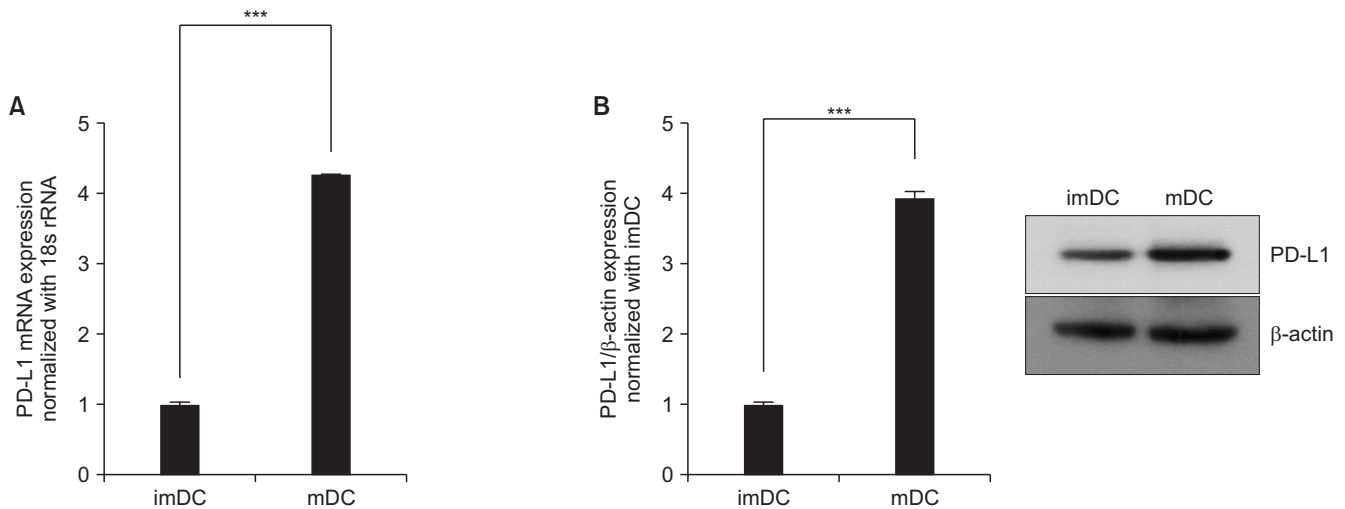


**Fig. 2.** mDCs express high PD-L1 levels. On Day 5, DCs were cultured with LPS (1  $\mu$ g/mL) for mDC or control medium-only for imDC. (A) The relative PD-L1 mRNA level was quantified by real-time PCR, and its expression was normalized to 18s rRNA. All qRT-PCR data represent the mean $\pm$ standard error of the mean of three biological replicates. (B) Western blot analysis of PD-L1 protein levels was performed using PD-L1 antibodies, and  $\beta$ -actin was used as a loading control. \*\*\* $p$ <0.001, compared with imDC. mDCs, mature dendritic cells; imDC, immature dendritic cell; PD-L1, programmed death ligand 1; LPS, lipopolysaccharide; mRNA, messenger RNA; PCR, polymerase chain reaction; rRNA, ribosomal RNA; qRT-PCR, quantitative reverse transcription-polymerase chain reaction.

ing lymphocytes at a 1:10 DC ratio, and co-cultured for five days. Next, the cell proliferation assay was accomplished by Celltiter Glo<sup>®</sup> luminescent assay (Promega). The plate was incubated for 10 minutes, and signals were measured on a VICTOR X3 luminometer (PerkinElmer). Data represents the comparison between DC-induced lymphocyte and lymphocyte-only proliferation.

## 8. Interferon-gamma detection through enzyme-linked immunosorbent (ELISpot) assays

The ELISpot assay was implemented to detect and count single cells that secreted interferon-gamma (IFN- $\gamma$ ) protein *in vitro* upon antigen exposure. The mouse IFN- $\gamma$  ELISpot assay kits were purchased from AID and used adhering to the manufacturer's instructions. Splenocytes from TRAMP-C1 tumor-bearing mice with or without DC treatment were *in vitro* stimulated with tumor cell lysates on a precoated 96-well plate. The plate was incubated for 18 hours in a 5% CO<sub>2</sub> atmosphere at 37°C. After cells were washed and fixed, a detection antibody was added to each well, incubated for 2 hours at room temperature with an alkaline phosphatase conjugate, and developed with a BCIP/NBT substrate solution (Mabtech). Visible spots were counted using an automated AID ELISpot reader (AID).

## 9. Immunohistochemistry (IHC)

IHC assays detected immune cells and mono-DC treatment differences. Tumor tissues were fixed with 10% neu-

tral buffered formalin at room temperature for 18 to 24 hours. After fixation, tumor tissues were rinsed, dehydrated, and embedded in paraffin blocks. The tumors' paraffin-embedded sections were stained with anti-CD8 and probed with a horseradish peroxidase-labeled secondary antibody (Dako). These sections were then stained with 3,3-diaminobenzidine tetrahydrochloride (DAB; Dako), dehydrated, and mounted.

## 10. Statistical analysis

Data represent the mean $\pm$ standard deviation of at least three independent experiments, and statistical analysis was performed using one-way ANOVA; a  $p$ <0.05 was considered statistically significant. Group means were compared using the unpaired *t*-test and were statistically significant at a  $p$ <0.05. Results were analyzed using the Prism version 8.00 (GraphPad Software).

# RESULTS

## 1. Specific and efficient siRNA-mediated PD-L1-knockdown in cultured DCs

On Day 5, relative mRNA PD-L1 and protein levels in matured DCs increased by 4.26-fold and 3.94-fold compared to immature DCs, with statistical significance ( $p$ <0.001) (Fig. 2). In addition, the off-target knockdown effects on mRNA and protein levels were examined to determine siRNA's specificity and efficacy in silencing PD-L1 expression in monocyte-derived DCs. Immature DCs were transfected with or without 0.1 nmol siRNA and cultured in a matura-



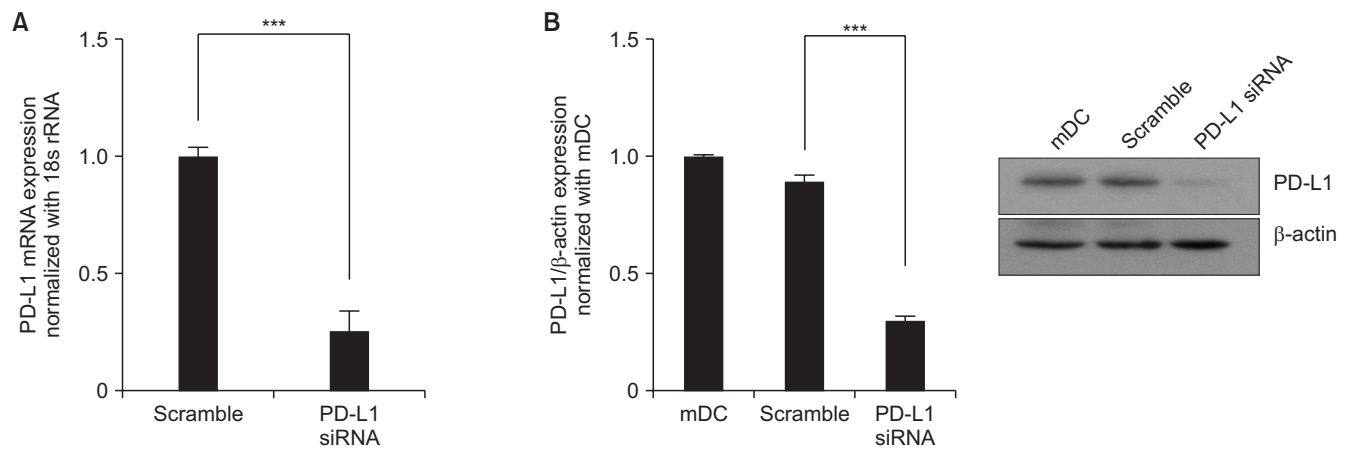


**Fig. 3.** PD-L1-knockdown mDCs. Immature DCs were transiently transfected with PD-L1 or negative-control siRNA duplexes and pulsed with cell lysates or PSMA peptides. After 24 hours, PD-L1 knockdown DCs were cultured in a maturation medium containing LPS (1  $\mu$ g/mL). (A) Relative PD-L1 mRNA levels were quantified using real-time PCR, and expressions were normalized to 18s rRNA. All qRT-PCR data represent the mean  $\pm$  standard error of the mean of three biological replicates. (B) Western blot analysis determined PD-L1 protein levels in mature DCs, and  $\beta$ -actin was used as a loading control. \*\*\* $p$ <0.001, compared with mDC transfected with scramble siRNA control. PD-L1, programmed death ligand 1; mDCs, mature dendritic cells; siRNA, small interfering RNA; PSMA, prostate specific membrane antigen; DCs, dendritic cells; LPS, lipopolysaccharide; mRNA, messenger RNA; PCR, polymerase chain reaction; rRNA, ribosomal RNA; qRT-PCR, quantitative reverse transcription-polymerase chain reaction.

tion medium containing IL-4 and GM-CSF. PD-L1 siRNA transfection decreased PD-L1 mRNA and protein levels 48 hours post-transfection, whereas negative control (scrambled) siRNA transfection had no significant effect; mRNA and protein levels decreased by 0.25-fold and 0.34-fold compared to the scrambled siRNA control ( $p$ <0.001) (Fig. 3). Various maturation and costimulatory molecules' mRNA levels were examined two days post-transfection to verify that the targeted PD-L1 siRNA did not affect DC maturation or prompt other off-target effects. The data substantiated that no molecules were affected by the tested siRNA and that siRNA DC transfection can precisely and efficiently silence PD-L1.

## 2. Characterization of mouse myeloid-DCs derived from bone marrow (BM) cells

Ag-pulsed and transfected PD-L1 Mono-DC originating from mouse BM cells' efficacy was evaluated using a subcutaneous TRAMP-C1 mouse prostate cancer model. DCs from BM-derived mouse monocytes pulsed with prostate cancer tumor antigens demonstrated characteristics. After DC cultures and transfection, GM-CSF and IL-4 treatment combined with tumor cell lysates and PSMA peptide pulsing yielded DCs with typical mature DC morphologies: enlarged cytoplasm, dendritic extensions, and a round nucleus with visible nucleoli (Fig. 4A). Despite treatment, the DCs' cellular morphology remained similar to that of untreated DCs.

Flow cytometry analysis of differentiated DCs revealed cell surface marker expressions of CD11c, CD80, CD86, MHC I, and MHC II (Fig. 4B). In addition, T-cells were co-cultured

with mature PD-L1-knockdown DCs for five days to investigate whether specific siRNA knockdown increased DCs' stimulatory capacity. After siRNA PD-L1 transfection, treated DCs were pulsed with tumor cell lysate antigens. Upon exposure to A, T-cell proliferation increased by more than 2-fold compared to unstimulated T-cells (Fig. 4C). These results indicate that siRNA PD-L1 transfection followed by antigen pulsing enhances T-cell proliferation, enhancing the immune response against tumor cells.

## 3. PD-L1-knockdown DCs' therapeutic efficacy

The potential treatment efficacy was examined using the TRAMP-C1 prostate cancer C57BL/6 mouse model over four weeks post-subcutaneous cancer cell injection. The mice were randomly allocated into the following groups ( $n=5$  mice/group): vehicle control (without DCs, saline), no pulsed Ag DCs, TRAMP-C1 cell lysate-pulsed DCs, and PSMA peptide-pulsed DCs. Mice were subcutaneously injected with PD-L1-knockdown DCs around inguinal lymph nodes once a week for three weeks. DC treatment in TRAMP-C1-injected mice decreased tumor volume compared to the saline-treated group (TGI 90.9%,  $p=0.002$ ; mature DC [mDC] group, 80.5%;  $p=0.0022$ ; mDC siRNA PD-L1 pulsed cell lysates and 90.5%;  $p=0.008$ ; mDC siRNA PD-L1 pulsed PSMA peptide, respectively) (Fig. 5A). However, no statistical significance was noted between the with or without antigen pulsing groups. Despite the lack of significant differences, histological alterations were observed from the H&E and CD8 stained sections. In the DC-treated group, tumor volume was consider-

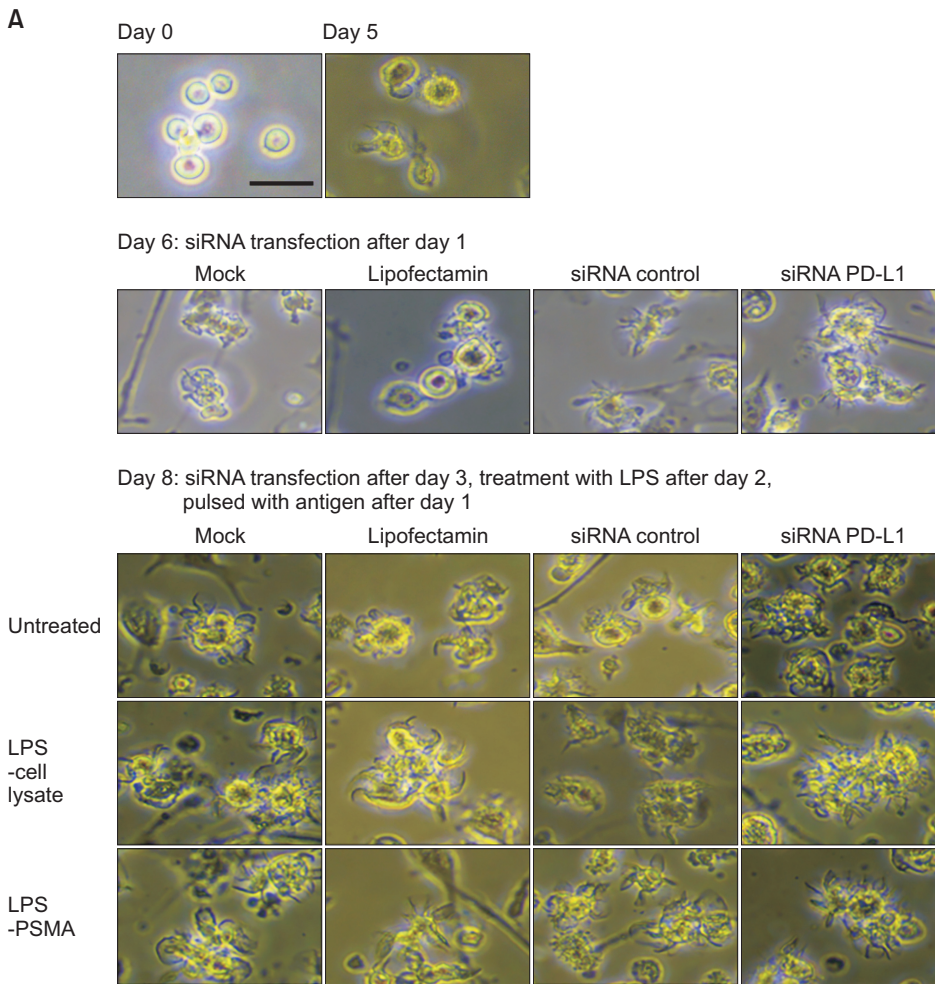


**Fig. 4.** Characterization of PD-L1 knockdown mDCs derived from BM cells pulsed with prostate cancer tumor antigens. (A) Differentiated DCs images after BM cell cultures were treated with GM-CSF and IL-4 and pulsed with tumor cell lysates or PSMA peptides. Scale bar=20 μm. (B) Flow cytometric analysis of differentiated DCs to determine DC-specific cell surface marker expressions. (C) T-cell proliferation (MLR assay) with mDCs in the presence or absence of tumor antigen demonstrated a significant difference compared with T-cells-only. PD-L1, programmed death ligand 1; mDCs, mature dendritic cells; BM, bone marrow; DCs, dendritic cells; GM-CSF, granulocyte-macrophage colony-stimulating factor; IL-4, interleukin-4; PSMA, prostate specific membrane antigen; MLR, mixed lymphocyte reaction; siRNA, small interfering RNA; LPS, lipopolysaccharide; imDC, immature dendritic cell; RLU, relative light units.

ably reduced (9.1%;  $p=0.024$ ; mDC group, 19.5%;  $p=0.024$ ; mDC siRNA PD-L1 pulsed cell lysates, and 9.4%;  $p=0.012$ ; mDC siRNA PD-L1 pulsed PSMA peptide, respectively). No body weight differences relative to the pulsing type were noted among DC-treated groups (Fig. 5B).

**4. Significant effects from Ag-specific T-cell immune responses with PD-L1 knockdown DCs**

Effector T-cells were collected from the splenocytes of TRAMP-C1 tumor-bearing mice to verify whether antigen-pulsed PD-L1-knockdown DCs induced systemic anti-tumor immunity. The ELISpot assay was used to analyze and count IFN- $\gamma$  secreting CD8+ T-cells to quantify these effects. The PD-L1-knockdown DC group’s IFN-  $\gamma$  secreting CD8+ T-cell frequency was significantly higher than those without Ag-pulsing. The cell lysate-pulsing group exhibited considerably increased IFN- $\gamma$  spot prevalence than the vehicle control (mean values: vehicle, 5.78; mDC, 61.83; mDC siRNA PD-L1 cell lysate, 172; mDC siRNA PD-L1 PSMA, 206.17;  $p<0.001$ ) (Fig. 6A). Similarly, the PSMA peptide pulsing group expressed a statistically significant increase in IFN- $\gamma$  spot

counts (mean values: vehicle, 44.33; mDC, 121; mDC siRNA PD-L1 cell lysate, 204.67; mDC siRNA PD-L1 PSMA, 233;  $p<0.001$ ). These results establish that PD-L1-knockdown/Ag pulsing group converted naïve T-cells to effector T-cells, regressing the residual tumor. Therefore, these therapeutic responses were associated with the induction of IFN- $\gamma$ -secreting CD8+ T-cells. Lastly, IHC staining was completed to confirm the immune cell distribution of those recruited in response to the tumor (Fig. 6B). Notably, CD8 expression levels were significantly higher in the PSMA peptide-pulsed PD-L1-knockdown DC group.

**DISCUSSION**

Chimeric antigen receptor (CAR) T-cell immunotherapy using genetically modified T-cells directly from the patient has revealed revolutionary clinical responses concerning hematologic malignancy [13]. A phase 1 CAR T application trial on prostate cancer displayed no severe toxicities, and prostate specific antigen (PSA) decline in six patients [14]. As such, genetic engineering techniques are progressing

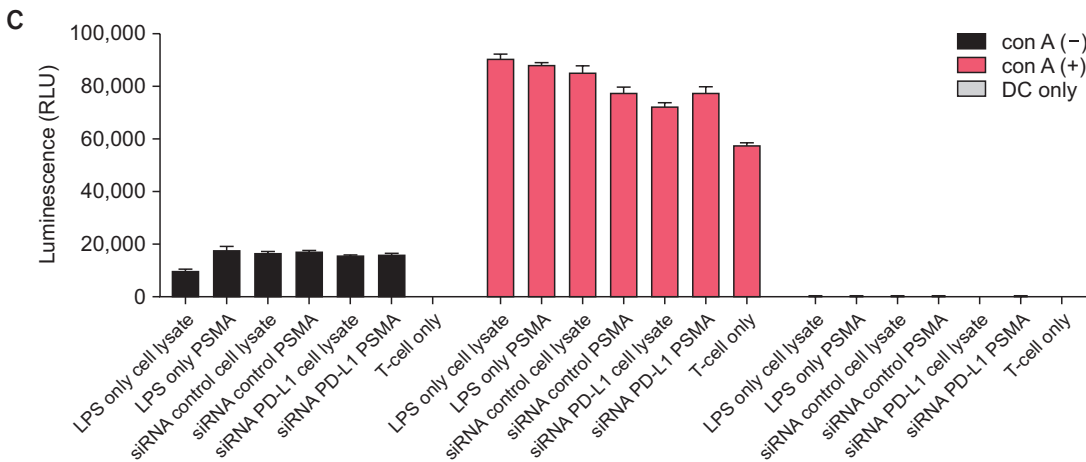
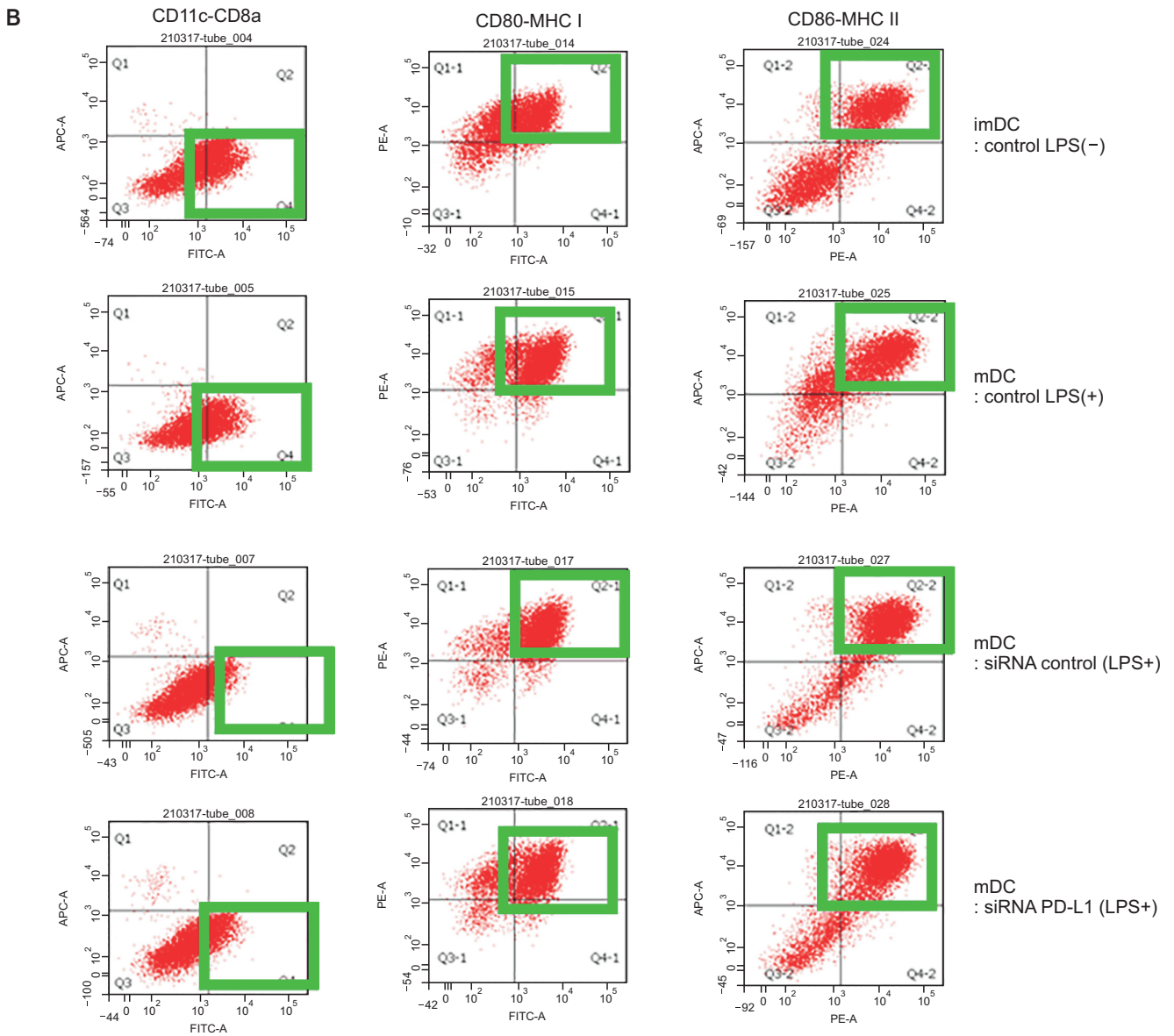
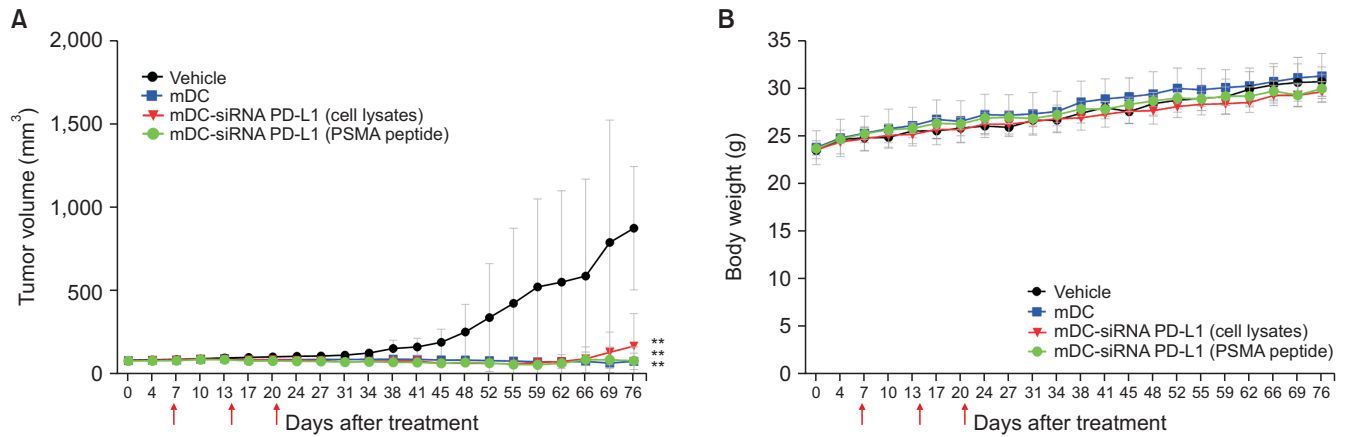


Fig. 4. Continued.



**Fig. 5.** siRNA PD-L1 DC therapeutic efficacy in TRAMP-C1 tumor cells with prostate cancer. TRAMP-C1-bearing tumor mice were subcutaneously injected around inguinal lymph nodes once a week for three weeks with  $5 \times 10^6$  DCs for the medium group. (A) Tumor volume. (B) Body weight. The data represent the mean  $\pm$  standard deviation. Compared with the vehicle group, all treated mice indicated reduced tumor volumes (\*\* $p < 0.01$ ). siRNA, small interfering RNA; PD-L1, programmed death ligand 1; DCs, dendritic cells; mDCs, mature dendritic cells; PSMA, prostate specific membrane antigen.

closer to clinical use. Thus, our study explores genetically engineered DCs for prostate cancer therapy. PD-L1 targeting genes in recombinant DCs verified their inhibitory power and specificity in an *in vivo* prostate cancer mouse model.

Trials employing DCs in prostate cancer treatments are still ongoing. For example, in a ProVENT (NCT03686683) trial, sipuleucel-T prevented Gleason-grade aggravation during active observation [15]. Tryggstad et al. [16] reported in a phase 1/2 study that adjuvant DC treatment in high-risk prostate cancer patients after radical prostatectomy reduced biochemical recurrence without side effects. Additional radiation therapy before sipuleucel-T did not help humoral and cellular responses in metastatic CRPC [17]. In a phase 1 study on metastatic CRPC, an ipilimumab and sipuleucel-T combination was verified as safe as it increased specific immunoglobulins levels [18]. Although only a few patients were treated, the authors anticipate DC to be effective in each prostate cancer stage.

Tumor microenvironments are surrounded by immune cells, stromal cells, the extracellular matrix, and cytokines that prostate cancer cells can interact with to upregulate PD-L1 expression [19]. Prostate cancer often exhibits low lymphocytic infiltration, and T-cells are detected more commonly in benign stroma than in cancer [20]. Stromal-derived factors transform monocytes into PD-L1-overexpressed immunosuppressive DCs, which lose their ability to present tumor antigens to T-cells [21]. Stromal and tumor cells secrete interleukin-6 and activate signal transducer and activator of transcription (STAT) 3, upregulating PD-L1 on DCs and diminishing anti-tumor immunity [21,22]. Therefore, the tumor microenvironments surrounding prostate cancer are consid-

ered immunosuppressive barriers for immune degradation, including DC function. Recombinant DCs efficiently present antigens, activate, migrate to lymph nodes, interact with T cells, and initiate and regulate adaptive immune responses. Their superior ability to move through lymph nodes is crucial for activating the immune system. This characteristic aligns well with our research goal to enhance the therapeutic effect of prostate cancer treatments; thus, recombinant DCs were selected for this study.

Immunity-enhanced DCs are needed to break through this tumor microenvironment barrier; thus, we designed a PD-L1-knockdown mature DC treatment. Mature DCs have increased protruded dendrites (Fig. 3), can stimulate T-cells, and migrate [23]. Notably, mature DCs exhibited superior immunologic responses and clinical results in melanoma than immature DC [24]. Unfortunately, no gold standard for effective DC maturation exists. Therefore, we used LPS gram-negative bacterial endotoxins (potent inflammatory mediators) [25], polyinosinic-polycytidylic acid (a synthetic double-stranded RNA analog that induces stable maturation of functionally active DCs) [26], and a cocktail maneuver including various cytokines [27]. Ultimately, we confirmed that the matured DCs effectively activated T cells specific to certain antigens through IFN- $\gamma$  secretion.

Concurrently, the antigen type loaded on DCs also influences the treatment's effect. Short peptides are easily added to culture media and presented on DC's MHC class 1 [28,29]; however, short peptides are limited because they incorporate CD4+ T-cells with less expansion and memory [29,30]. Loading whole proteins to DCs can stimulate MHC classes 1 and 2, but this cannot cover more immunogenic mutations of



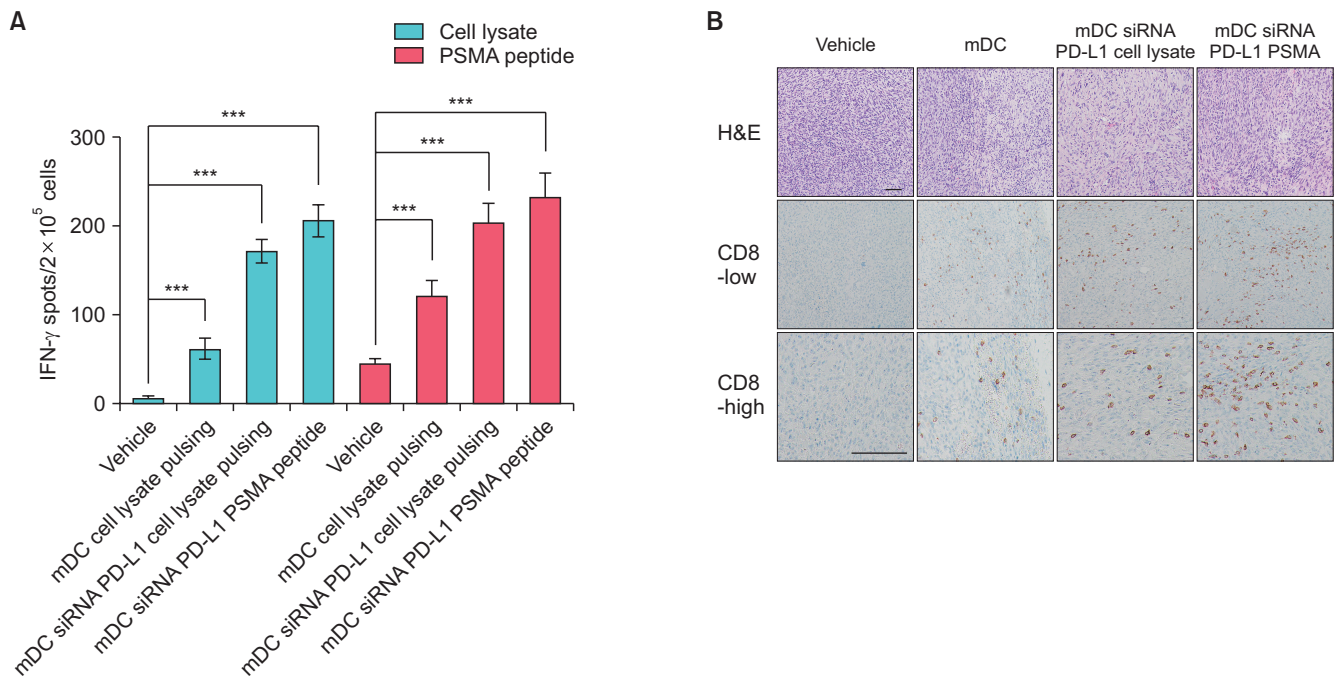


**Fig. 6.** Induced tumor-specific immune response. Immune responses in tumor tissues were evaluated after mDC treatment in the vehicle, mDC, siRNA PD-L1 mDC pulsed cell lysates, and siRNA PD-L1 mDC pulsed PSMA peptide groups. (A) The ELISpot assay was performed to quantify IFN- $\gamma$  secreting CD8+ T-cells (\*\* $p < 0.001$  for all groups compared to the vehicle). (B) IHC staining was conducted to verify immune cell distributions recruited in response to the tumor. Scale bar=50  $\mu$ m. CD8-low, CD8 stain with 200 $\times$  magnification; CD8-high, CD8 stain with 800 $\times$  magnification. mDCs, mature dendritic cells; siRNA, small interfering RNA; PD-L1, programmed death ligand 1; PSMA, prostate specific membrane antigen; IFN- $\gamma$ , interferon-gamma; IHC, immunohistochemistry; PSMA, prostate specific membrane antigen.

polymorphous tumor conditions [29]. Alternatively, clinically used proteins such as PSA, PSMA, and prostatic acid phosphatase (PAP) are also expressed in the patient's cell and are related to immune tolerance [29]. Tumor cell lysates, including cell membrane fragments, RNA, and DNA, are more immunogenic [29]. However, obtaining sufficient patient tumor samples may be difficult in clinical situations and demand extra cost. We used PSMA and cell lysates as antigens for DC; both antigens expressed specific T-cell immune responses, PSMA cross-reactions, and verified tumor lysates.

Our study has some limitations. First, applying these results directly to humans is challenging. We used a syngeneic heterotopic CRPC mouse model. As mice DCs affect the mouse's immune system, we could not select humanized or athymic mice samples. Second, non-recombinant DCs also exhibited excellent TGI, similar to recombinant DCs. We injected DCs at the groin lymph node furthest from the tumor lesion as DCs or T-cells moved from the injection site to the tumor using the mouse's immune reaction. Although the infiltrated lymphocytes were more prevalent in the recombinant DC group, TGI was substantial in both non-recombinant and recombinant DC groups. DCs specifically detect and present antigens, modulating immune responses. This ability minimizes reactions to normal cells while en-

hancing immune responses against abnormal cells, such as tumor cells, thereby reducing side effects. DCs also form immune memory, enabling them to respond to previously encountered antigens. DCs demonstrate effectiveness in tumor therapy through various aspects, including specificity, immune memory, and regulatory functions. Our *in vivo* study results corroborate these observations. The selection of siRNAs was based on their rapid intracellular degradation, resulting in fewer side effects and higher specificity during gene regulation. However, the similarity in results between DCs and recombinant DCs suggests that the effects of siRNA may not be sustained. Therefore, additional experiments, such as those incorporating short hairpin RNA, are necessary to investigate the persistence of these therapeutic effects.

## CONCLUSIONS

Our developed monocyte-derived DCs transfected with PD-L1 siRNA from mouse BM effectively inhibited tumor growth in an *in vivo* mouse model. These recombinant DCs increased antigen-specific immune responses, evidencing therapeutic and preventative effects on CRPC models. Our study highlights that PD-L1 inhibition in DCs increases



antigen-specific immune responses and provides promising methods for enhancing current prostate cancer immunotherapy treatments.

## CONFLICTS OF INTEREST

The authors have nothing to disclose.

## FUNDING

This work was supported by the National Research Foundation of Korea (NRF) grant funded by the Korean government (MSIT) (No. NRF-2020R1C1C1008101 & NRF-2023R1A2C1003830).

## ACKNOWLEDGMENTS

This paper was selected for the Best Paper Award at the 75th Annual Meeting of the Korean Urological Association in 2023.

## AUTHORS' CONTRIBUTIONS

Research conception and design: Se Young Choi and Yunlim Kim. Data acquisition: Se Young Choi, Yunlim Kim, and Chung Beum Wee. Statistical analysis: Yunlim Kim. Data analysis and interpretation: Se Young Choi, Yunlim Kim, and Bumjin Lim. Drafting of the manuscript: Se Young Choi and Yunlim Kim. Critical revision of the manuscript: In Ho Chang and Choung-Soo Kim. Obtaining funding: Se Young Choi and Yunlim Kim. Administrative, technical, or material support: Yunlim Kim and Se Young Choi. Supervision: Choung-Soo Kim. Approval of the final manuscript: all authors.

## REFERENCES

1. Siegel RL, Miller KD, Fuchs HE, Jemal A. Cancer statistics, 2022. *CA Cancer J Clin* 2022;72:7-33.
2. Yamada Y, Beltran H. The treatment landscape of metastatic prostate cancer. *Cancer Lett* 2021;519:20-9.
3. Alatrash G, Jakher H, Stafford PD, Mittendorf EA. Cancer immunotherapies, their safety and toxicity. *Expert Opin Drug Saf* 2013;12:631-45.
4. Motzer RJ, Tannir NM, McDermott DF, Arén Frontera O, Melichar B, Choueiri TK, et al. Nivolumab plus ipilimumab versus sunitinib in advanced renal-cell carcinoma. *N Engl J Med* 2018;378:1277-90.
5. Wolchok JD, Chiarion-Sileni V, Gonzalez R, Rutkowski P,

## Recombinant dendritic cells for prostate cancer therapy

- Grob JJ, Cowey CL, et al. Overall survival with combined nivolumab and ipilimumab in advanced melanoma. *N Engl J Med* 2017;377:1345-56.
6. Chen DS, Mellman I. Oncology meets immunology: the cancer-immunity cycle. *Immunity* 2013;39:1-10.
  7. Lu S, Stein JE, Rimm DL, Wang DW, Bell JM, Johnson DB, et al. Comparison of biomarker modalities for predicting response to PD-1/PD-L1 checkpoint blockade: a systematic review and meta-analysis. *JAMA Oncol* 2019;5:1195-204.
  8. Cao J, Yang X, Chen S, Wang J, Fan X, Fu S, et al. The predictive efficacy of tumor mutation burden in immunotherapy across multiple cancer types: a meta-analysis and bioinformatics analysis. *Transl Oncol* 2022;20:101375.
  9. Abida W, Cheng ML, Armenia J, Middha S, Autio KA, Vargas HA, et al. Analysis of the prevalence of microsatellite instability in prostate cancer and response to immune checkpoint blockade. *JAMA Oncol* 2019;5:471-8.
  10. Stultz J, Fong L. How to turn up the heat on the cold immune microenvironment of metastatic prostate cancer. *Prostate Cancer Prostatic Dis* 2021;24:697-717.
  11. Kantoff PW, Higano CS, Shore ND, Berger ER, Small EJ, Penson DE, et al. Sipuleucel-T immunotherapy for castration-resistant prostate cancer. *N Engl J Med* 2010;363:411-22.
  12. Palucka K, Banchereau J. Cancer immunotherapy via dendritic cells. *Nat Rev Cancer* 2012;12:265-77.
  13. June CH, O'Connor RS, Kawalekar OU, Ghassemi S, Milone MC. CAR T cell immunotherapy for human cancer. *Science* 2018;359:1361-5.
  14. Junghans RP, Ma Q, Rathore R, Gomes EM, Bais AJ, Lo AS, et al. Phase I trial of anti-PSMA designer CAR-T cells in prostate cancer: possible role for interacting interleukin 2-T cell pharmacodynamics as a determinant of clinical response. *Prostate* 2016;76:1257-70.
  15. Ross A, Armstrong AJ, Pieczonka CM, Bailen JL, Tutrone RF, Cooperberg MR, et al. A comparison of sipuleucel-T (sip-T) product parameters from two phase III studies: PROVENT in active surveillance prostate cancer and IMPACT in metastatic castrate-resistant prostate cancer (mCRPC). *J Clin Oncol* 2020;38:321.
  16. Tryggstad AMA, Axcrone K, Axcrone U, Bigalke I, Brennhovd B, Inderberg EM, et al. Long-term first-in-man phase I/II study of an adjuvant dendritic cell vaccine in patients with high-risk prostate cancer after radical prostatectomy. *Prostate* 2022;82:245-53.
  17. Twardowski P, Wong JYC, Pal SK, Maughan BL, Frankel PH, Franklin K, et al. Randomized phase II trial of sipuleucel-T immunotherapy preceded by sensitizing radiation therapy and sipuleucel-T alone in patients with metastatic castrate resistant prostate cancer. *Cancer Treat Res Commun* 2019;19:100116.

18. Scholz M, Yep S, Chancey M, Kelly C, Chau K, Turner J, et al. Phase I clinical trial of sipuleucel-T combined with escalating doses of ipilimumab in progressive metastatic castrate-resistant prostate cancer. *Immunotargets Ther* 2017;6:11-6.
19. Yu P, Steel JC, Zhang M, Morris JC, Waitz R, Fasso M, et al. Simultaneous inhibition of two regulatory T-cell subsets enhanced interleukin-15 efficacy in a prostate tumor model. *Proc Natl Acad Sci U S A* 2012;109:6187-92.
20. Rådestad E, Egevad L, Jorns C, Mattsson J, Sundberg B, Nava S, et al. Characterization of infiltrating lymphocytes in human benign and malignant prostate tissue. *Oncotarget* 2017;8:60257-69.
21. Palicelli A, Croci S, Bisagni A, Zanetti E, De Biase D, Melli B, et al. What do we have to know about PD-L1 expression in prostate cancer? A systematic literature review. Part 3: PD-L1, intracellular signaling pathways and tumor microenvironment. *Int J Mol Sci* 2021;22:12330.
22. Zou S, Tong Q, Liu B, Huang W, Tian Y, Fu X. Targeting STAT3 in cancer immunotherapy. *Mol Cancer* 2020;19:145.
23. De Vries IJ, Krooshoop DJ, Scharenborg NM, Lesterhuis WJ, Diepstra JH, Van Muijen GN, et al. Effective migration of antigen-pulsed dendritic cells to lymph nodes in melanoma patients is determined by their maturation state. *Cancer Res* 2003;63:12-7.
24. de Vries IJ, Lesterhuis WJ, Scharenborg NM, Engelen LP, Ruiter DJ, Gerritsen MJ, et al. Maturation of dendritic cells is a prerequisite for inducing immune responses in advanced melanoma patients. *Clin Cancer Res* 2003;9:5091-100.
25. Griffiths KL, Tan JK, O'Neill HC. Characterization of the effect of LPS on dendritic cell subset discrimination in spleen. *J Cell Mol Med* 2014;18:1908-12.
26. Verdijk RM, Mutis T, Esendam B, Kamp J, Melief CJ, Brand A, et al. Polyribonucleosinic polyribocytidylic acid (poly(I:C)) induces stable maturation of functionally active human dendritic cells. *J Immunol* 1999;163:57-61.
27. Massa C, Thomas C, Wang E, Marincola F, Seliger B. Different maturation cocktails provide dendritic cells with different chemoattractive properties. *J Transl Med* 2015;13:175.
28. Murphy G, Tjoa B, Ragde H, Kenny G, Boynton A. Phase I clinical trial: T-cell therapy for prostate cancer using autologous dendritic cells pulsed with HLA-A0201-specific peptides from prostate-specific membrane antigen. *Prostate* 1996;29:371-80.
29. Sutherland SIM, Ju X, Horvath LG, Clark GJ. Moving on from sipuleucel-T: new dendritic cell vaccine strategies for prostate cancer. *Front Immunol* 2021;12:641307.
30. Janssen EM, Lemmens EE, Wolfe T, Christen U, von Herrath MG, Schoenberger SP. CD4+ T cells are required for secondary expansion and memory in CD8+ T lymphocytes. *Nature* 2003;421:852-6.